Available online at www.sciencedirect.com
SCIENCE DIRECT
Catalysis Today 114 (2006) 86–93
CATALYSIS TODAY
www.elsevier.com/locate/cattod

Effects of Ba loading and calcination temperature on $BaAl_2O_4$ formation for BaO/Al_2O_3 NO_x storage and reduction catalysts

Tamás Szailer [a], Ja Hun Kwak [a], Do Heui Kim [a], János Szanyi [a], Chongmin Wang [b], Charles H.F. Peden [a,*]

[a] Institute for Interfacial Catalysis, Pacific Northwest National Laboratory, P.O. Box 999, MSIN: K8–93, Richland, WA 99352, USA
[b] Environmental Molecular Sciences Laboratory, Pacific Northwest National Laboratory, P.O. Box 999, MSIN: K8-93, Richland, WA 99352, USA

Available online 23 March 2006

Abstract

The effect of thermal treatment on the structure and chemical properties of Ba-oxide-based NO_x storage/reduction catalysts with different Ba loadings was investigated using BET, TEM, EDS, TPD and FT-IR techniques. On the basis of the present and previously reported results, we propose that moderate (<∼873 K) temperature calcinations result in a single monolayer (ML) 'coating' of BaO on the alumina surface. At high Ba loading in excess of that required for a full monolayer 'coating' (>8 wt.% BaO), small (∼5 nm) particles of 'bulk' BaO are present on top of the one ML BaO/Al_2O_3 surface. We did not observe any detectable morphological changes upon higher temperature thermal treatment of 2 and 8 wt.% BaO/Al_2O_3 samples, while dramatic changes occurred for the 20 wt.% sample. In this latter case, the transformations included $BaAl_2O_4$ formation at the expense of the bulk BaO phase. In particular, we conclude that the surface (ML) BaO phase is quite stable against thermal treatment, while the bulk phase provides the source of Ba for $BaAl_2O_4$ formation.

Keywords: BaO/Al_2O_3; NO_x Storage/reduction; Catalyst morphology

1. Introduction

Operating internal combustion engines under net oxidizing conditions is desirable to increase fuel efficiency. This mode of engine operation, however, makes traditional three-way catalysts (TWC) ineffective for the reduction of NO_x in the exhaust gas stream. In the last decade new approaches toward NO_x reduction in oxygen-rich environments have been explored with one of the most promising being the NO_x storage/reduction (NSR) technology [1] (also known as lean-NO_x traps (LNTs) and NO_x adsorber catalysts). Barium oxide-based materials (in particular $Pt/BaO/Al_2O_3$) have proven to be highly efficient NO_x storage/reduction catalysts.

The fundamentals of NO_x uptake/release processes have been studied extensively on catalysts based on BaO on alumina support materials. Studies using vibrational spectroscopic techniques (IR and Raman) and temperature-programmed desorption (TPD) have been aimed at understanding the chemical nature of the NO_x species formed on/in these catalysts [2–5]. The formation of different NO_x species on the active BaO phase has been clearly shown in the first of these studies; however, detailed assignments of the spectra to specific BaO morphologies has only recently been proposed [5]. For example, in TPD studies two distinct NO_x desorption features were reported; one at lower temperature (∼693 K with the release of NO_2), and another at higher temperature (∼800 K resulting in the desorption of $NO + O_2$). These two desorption peaks have been shown to originate from the decomposition of monolayer and bulk barium nitrate phases, respectively. These assignments were made, in part, on the basis of the results of our recent ^{15}N NMR studies of NO_2 adsorption on BaO/Al_2O_3 samples [5]. We have observed separate Ba-associated nitrate species peaks at chemical shifts of 337 and 340.5 ppm. The intensity ratio of these two peaks varied with BaO coverage, and was clearly related to the intensity ratios of the NO_2 and NO desorption features in the NO_2 TPD spectra.

Extending the FT-IR and NMR spectroscopic studies with TEM and TP-XRD, we developed a 'morphology cycle' for BaO/Al_2O_3 during NO_x adsorption and release [6]. These results showed that large $Ba(NO_3)_2$ crystallites are formed on

* Corresponding author. Tel.: +1 509 376 1689; fax: +1 509 376 1044.
E-mail address: chuck.peden@pnl.gov (Charles H.F. Peden).

0920-5861/$ – see front matter © 2006 Elsevier B.V. All rights reserved.
doi:10.1016/j.cattod.2006.02.016

the alumina support during its typical preparation via incipient wetness impregnation with an aqueous solution containing dissolved $Ba(NO_3)_2$, and subsequent drying at low (<473 K) temperatures. A large fraction of the alumina surface remains Ba-free after this procedure. Upon higher (~773 K) temperature thermal treatment, these large $Ba(NO_3)_2$ crystallites decompose to form nanosized BaO particles. We proposed that a thin BaO film (monolayer) 'coating' forms on the alumina support and that the BaO nano-particles are located on top of this interfacial BaO layer. During room-temperature NO_2 uptake, nanosized (<5 nm) $Ba(NO_3)_2$ particles form. Heating the material to higher temperature (573 K) in the presence of NO_2 results in the formation of larger $Ba(NO_3)_2$ crystals (<15 nm). At still higher temperatures, and even in the absence of NO_2, the average particle size of $Ba(NO_3)_2$ crystallites increases further (<32 nm), and then, as $Ba(NO_3)_2$ decomposes, the nanosized BaO particles reform on top of the interfacial (monolayer, ML) BaO layer.

Effects of high temperature thermal degradation of NSR catalysts have been summarized recently by Epling et al. [1], and at least two reasons can be identified for concerns about these effects. During the rich conditions for NO_x reduction and catalyst regeneration, oxidation of hydrocarbons, CO and/or H_2 occurs. These reactions are highly exothermic and can result in local hot spots on the surface, potentially leading to thermal degradation. Perhaps more importantly, thermal deactivation is known to occur during processes implemented to remove sulfur from the NSR catalysts. Since $BaSO_4$ is thermodynamically more stable than Ba-nitrates and -carbonates, sulfur species (predominantly SO_2) in the engine exhaust are catalyst poisons for NSR operation. As such, various strategies that invariably use high temperature excursions have been developed to remove sulfur.

At least two deactivation modes have been proposed in the literature to explain performance degradation due to high temperature treatments. One is the formation of mixed metal oxides such as aluminates, zirconates, and titanates through the reaction of adsorbents and washcoat ingredients (alumina, zirconia, or titania). The formation of these new phases may then be responsible for reduced NO_x adsorption capacity [7]. The other is particle growth of either or both the precious metal and BaO storage material components of the NSR catalysts. For example, within a model that ''spill-over'' of NO_2 between the precious metal to the BaO sorbent material are critical processes in NO_x storage and reduction [1], particle growth would lead to a loss of interface between these components, thereby reducing spill-over rates.

In this work, we focused on the changes in the structure of model 2, 8, and 20 wt.% BaO/Al_2O_3 catalysts during calcinations to various temperatures, investigated by NO_2 adsorption and using FT-IR, TPD, TEM, and XRD.

2. Experimental

The BaO/Al_2O_3 NSR catalysts were prepared by the incipient wetness method, using an aqueous $Ba(NO_3)_2$ solution (Aldrich) and a γ-alumina support (200 m^2/g, Condea) to yield nominal 2, 8, and 20 wt.% BaO-containing samples. After impregnation, the catalysts were dried at 395 K and then 'activated' via a calcination at 773 K in flowing air for 2 h. To investigate thermal effects on the structure and NO_x adsorption properties of the samples, higher temperature calcinations were made in a muffle furnace for 2 h. The samples were sealed with parafilm and stored in a dry chamber to minimize carbonate formation.

The specific surface areas of the catalysts were determined by the BET method after nitrogen adsorption in an automated adsorption instrument (Micromeritics, TriStar). Prior to N_2 adsorption, all of the catalysts were flushed with N_2 at 523 K for 2 h and evacuated.

XRD analysis was carried out on a Philips PW3040/00 X'Pert powder X-ray diffractometer using the Cu Kα1 radiation (λ = 1.5406 Å) in step mode between 5 and 75° 2θ, with a step of 0.02°/s. Data analysis was accomplished using JADE (Materials Data Inc., Livermore, CA) as well as the Powder Diffraction File database (2003 Release, International Center for Diffraction Data, Newtown Square, PA).

TEM images were collected from BaO/Al_2O_3 samples calcined at 1273 K. TEM specimens were prepared by dusting the powder particles onto a carbon film-coated 200 mesh copper TEM grid. High-resolution TEM analysis was carried out on a JEOL JEM 2010 microscope with a specified point-to-point resolution of 0.194 nm. The operating voltage on the microscope was 200 keV. All images were digitally recorded with a slow scan CCD camera (image size 1024 × 1024 pixel), and image processing was carried out using a Digital Micrograph (Gatan). The composition of the particles was analyzed by energy-dispersive X-ray spectroscopy (EDS). The EDS spectrometer is an Oxford Link system and is attached onto the transmission electron microscope.

TPD experiments were carried out in a fixed-bed micro-catalytic quartz reactor. Calcined catalyst samples of 50 mg were pretreated at 873 K for 1 h and cooled to room temperature in flowing He prior to NO_2 adsorption experiments. All of the NO_2 adsorption experiments were conducted at 300 K using a 0.5% NO_2/He (99.999% purity, Matheson) gas mixture. After saturation, the catalysts were purged with He for 2 h and then the sample temperature was raised in a temperature-programmed fashion at 8 K/min to 973 K, while the evolved NO_x gases were monitored with a chemiluminescence NO_x analyzer (42C, Thermo Environmental). In this instrument, we measure [NO] and [total NO_x]. In illustrating these results, we will show spectra for the desorption of NO and NO_2 where the latter was obtained by subtracting the NO curve from the one for total NO_x (i.e., $[NO_2]$ = [total NO_x] − [NO]).

The infrared measurements were carried out in transmission mode, using a Mattson Research Series or Nicolet Magna-IR 750 spectrometer operating at 4 cm^{-1} resolution. The cell is connected to a gas handling/pumping station and, through both leak and gate valves, to a mass spectrometer (UTI 100C). The catalyst sample was pressed onto a fine tungsten mesh, which, in turn, was mounted onto a copper sample holder assembly attached to ceramic feedthroughs. This set up allowed heating of the samples to 1000 K and cooling to cryogenic temperatures. The sample temperature was monitored through a chromel/alumel thermocouple spot-welded to the top center of the tungsten mesh.

Table 1
Specific surface area of the catalysts

Calcination temperature (K)	Catalysts		
	2 wt.% BaO/Al_2O_3	8 wt.% BaO/Al_2O_3	20 wt.% BaO/Al_2O_3
	BET surface area (m^2/g)		
773	190.6	158.5	120.3
1073	159.6	149.1	110.1
1273	121.5	128.5	97.7

3. Results and discussion

3.1. Catalyst characterization

First, we measured the specific surface area by BET method as a function of Ba loading and calcination temperature with the results given in Table 1. Even for a standard calcination of 773 K, significant loss of the surface area was observed for the three samples studied here when the Ba loading was increased from 2 to 20 wt.%. At least some of this surface area loss may be accounted for by the filling of some of the pores of the alumina by the supported BaO phase which can occur to a greater extent as Ba loading increases. Increasing the calcination temperature results in a further loss of BET surface area for all catalysts regardless of the Ba loading.

Fig. 1 displays XRD patterns obtained for 2 wt.% (A), 8 wt.% (B), and 20 wt.% (C) BaO/Al_2O_3 samples calcined for 2 h at various temperatures between 773 and 1273 K. Also given in the figure are the published positions of the XRD peaks for BaO, γ-Al_2O_3, and $BaAl_2O_4$ crystalline phases. The results reveal that after calcination at 773 K no Ba-containing phase can be observed at any BaO loading. Baiker and coworkers [8] have obtained similar results and suggested that below 16.7% Ba loading the Ba-containing phase is amorphous. Utilizing synchrotron X-ray diffraction, however, we have been able to show [6] that 20 wt.% BaO/Al_2O_3 sample prepared as done in the present work contains small and broad diffraction peaks for a nano-particulate BaO phase with ~5 nm average particle size. Such small particles are not observable with typical laboratory

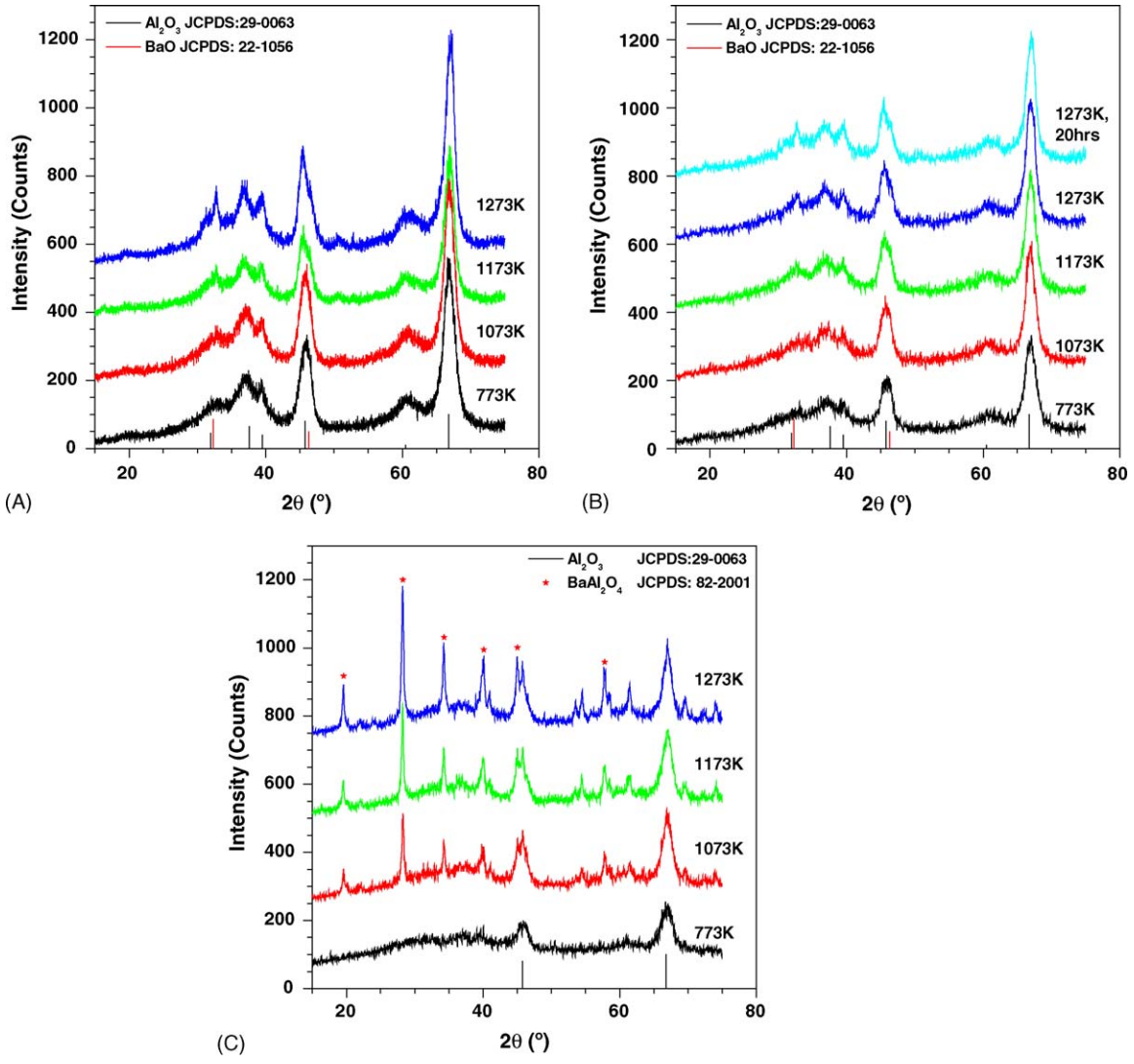

Fig. 1. XRD spectra of 2 wt.% (A), 8 wt.% (B), and 20 wt.% BaO/Al_2O_3 (C) NSR catalysts after calcination for 2 h to different temperatures.

XRD instrumentation. A further comparison of the diffraction patterns obtained for the 773 K-calcined samples reveals that the intensity of alumina peaks decreases with Ba loading due to attenuation of substrate alumina by the supported BaO phase. This suggests that the 'overlayer' BaO phase is relatively well dispersed over the alumina surface after a 773 K calcination, consistent with conclusions from our recent work [5,6].

Increasing the calcination temperature leads to only minor changes in the diffraction patterns for the 2 and 8 wt.% samples. Some sharpening of the alumina diffraction peaks is evident after a 1273 K calcination as expected by the loss of surface area described above. To see if a longer calcination time has any effect, the 8 wt.% sample was calcined for 20 h at 1273 K (data not shown). Even this vigorous treatment resulted in no further change in the XRD pattern (a result identical to that shown for 2 h at 1273 K as illustrated in Fig. 1B was obtained).

Dramatically different results were obtained for the 20 wt.% BaO/Al_2O_3 sample upon calcination. In this case, the diffraction patterns shown in Fig. 1C provide clear evidence that $BaAl_2O_4$ formation is detected at calcination temperatures as low as

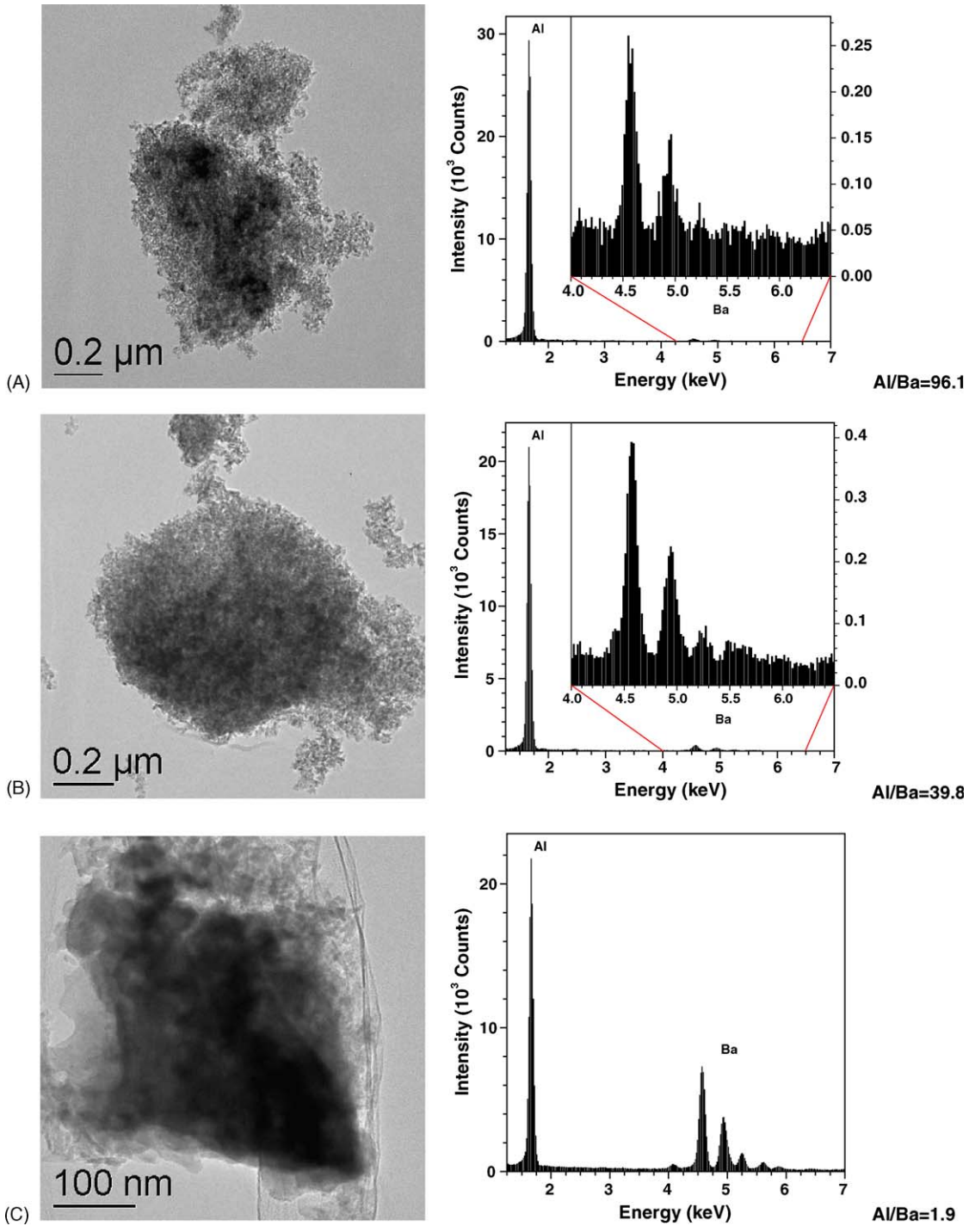

Fig. 2. TEM images and EDS spectra from 2, 8, and 20 wt.% BaO/Al_2O_3 calcined for 2 h at 1273 K.

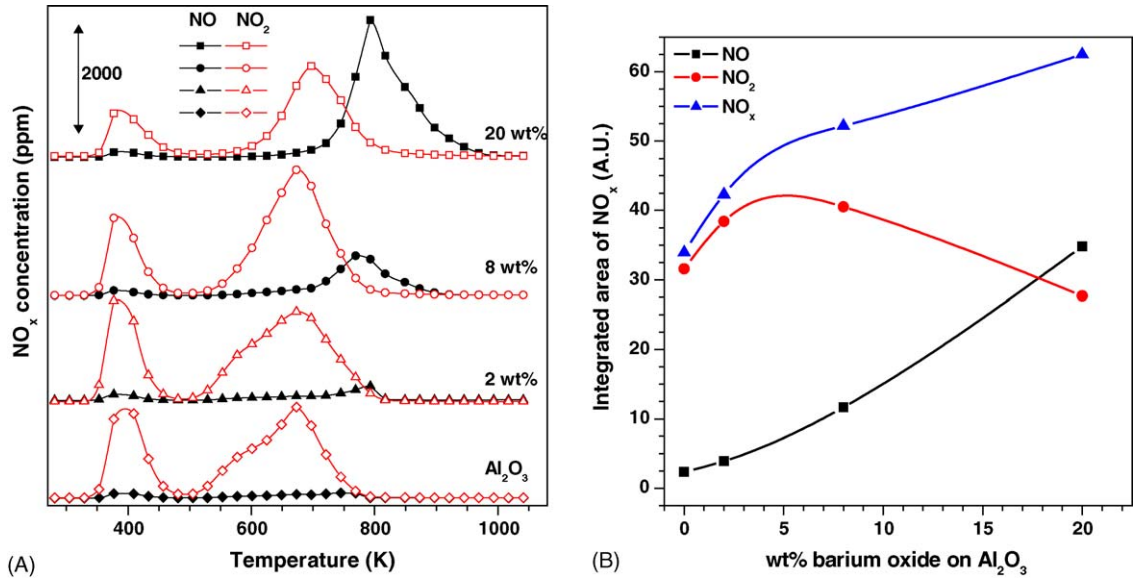

Fig. 3. TPD spectra obtained after 30 min NO_2 adsorption at room temperature on different Ba-loaded catalysts calcined at 773 K (A). Integration of the high (>473 K) TPD peaks (B).

1073 K, with the amount and crystallinity of this new phase increasing with the calcination temperature. It is interesting to note that although the Ba loading is high, no traces of a crystalline BaO phase is observed in the XRD data for this sample; rather, increasing the calcination temperature leads immediately to Ba-aluminate formation. From the shape and FWHM of the $BaAl_2O_4$ peaks it is evident that large (average size calculated to be ~50 nm) and highly crystalline particles are formed after the highest (1273 K) temperature calcination.

As additional evidence that $BaAl_2O_4$ formation is negligible for the 2 and 8 wt.% samples even after 1273 K calcinations, we obtained TEM micrographs from all catalysts after 2 h at 1273 K. Representative images are shown in Fig. 2 along with the corresponding EDS spectra obtained from the particles illustrated in the images. For the 20 wt.% sample (Fig. 2C), it was very easy to find dark, crystalline particles throughout the sample with the TEM. EDS results show that the Al/Ba atomic ratio for the particle shown in Fig. 2C is 1.92 consistent with the stoichiometry of $BaAl_2O_4$. Note that the size of this crystal is quite large, about 300 × 300 nm. For the 2 and 8 wt.% samples, we tried to find similar dark phases without success; rather, as in the representative images shown in Fig. 2A and B, there was nothing distinguishably different from images of the alumina support material itself. Consistent with this, Al/Ba ratios obtained from the corresponding EDS spectra for the 2 and 8 wt.% BaO/Al_2O_3 samples were considerably greater than 2, and became larger with decreasing Ba loading as expected.

In recently published work [5,6], we have proposed that BaO uniformly coats the alumina surface with a 'monolayer' (ML) phase upon synthesis that included an aqueous impregnation, elevated (~393 K) temperature drying and dry air calcination to 773 K. At BaO loadings greater than 1 ML (>~8 wt.%), nanometer-sized BaO particles form on top of the coating layer. Thus, the results reported here strongly suggest that the ML-phase is stable for even extended calcinations at quite high (1273 K) temperature, and that the source of Ba for formation of $BaAl_2O_4$ in the 20 wt.% sample is the Ba present in excess of that required to form a complete ML on the alumina surface. To investigate this further, we performed studies of the adsorption of NO_2 on these variously treated samples with TPD and FT-IR spectroscopy that we describe in the next section.

3.2. Interaction with NO_2

TPD spectra acquired after NO_2 adsorption at 300 K for Al_2O_3, and 2, 8, and 20 wt.% BaO/Al_2O_3 catalysts are shown in Fig. 3A. For the purposes of this paper, we only discuss the

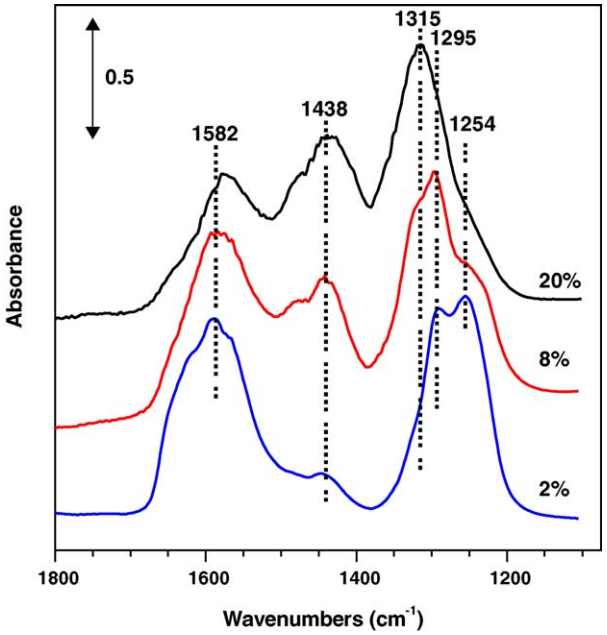

Fig. 4. IR spectra after NO_2 adsorption at room temperature on different Ba-loaded catalysts calcined at 773 K.

desorption peaks in the spectra that appear above 475 K because lower temperatures are not important for the practical operation of the NSR technology. These TPD spectra are very similar to what we have recently published [5,6] with additional data for the 2 wt.% sample included in this paper. There are two main high (>475 K) temperature desorption peaks, corresponding to NO_2 and NO desorption at ~600 and at ~800 K, respectively. These two desorption peaks have been proposed to originate from the decomposition of ML and bulk barium nitrate phases, respectively. Thus, it is especially notable in the spectra that the amount of NO desorption shows a strong correlation with Ba loading as this result provides strong evidence for this previous assignment. To be more quantitative, we calculated the peak areas above 475 K for these two desorption features and present the results in Fig. 3B. There it can be seen that, as just noted, the amount of desorbed NO (and NO_x) continuously increases with Ba loading. In contrast, the NO_2 desorption peak area is roughly constant (perhaps increases slightly) up to 8 wt.% Ba loading and then markedly decreases. Since the alumina surface is also known to adsorb NO_2 [1], the nearly constant NO_2 desorption peak area is expected for BaO 'coverages' up to a ML. At higher Ba loadings, the drop in the NO_2 TPD peak area can therefore be understood as arising from the covering of the ML BaO phase by the excess BaO.

The FT-IR spectra obtained from the 773 K-calcined 2, 8, and 20 wt.% BaO/Al_2O_3 after NO_2 exposure at 300 K, displayed in Fig. 4, can be understood in a similar way as the TPD results. The IR features observed are in accord with those reported previously [2,5,9,10]. On the Al_2O_3 support itself, two types of nitrates form upon NO_2 adsorption: so-called "bridging" (1234, 1250 cm^{-1} and 1595, 1620 cm^{-1}) and "chelating bidentate" (1300 and 1570 cm^{-1}) nitrates (this nomenclature is based on comparing ('fingerprinting') the peak

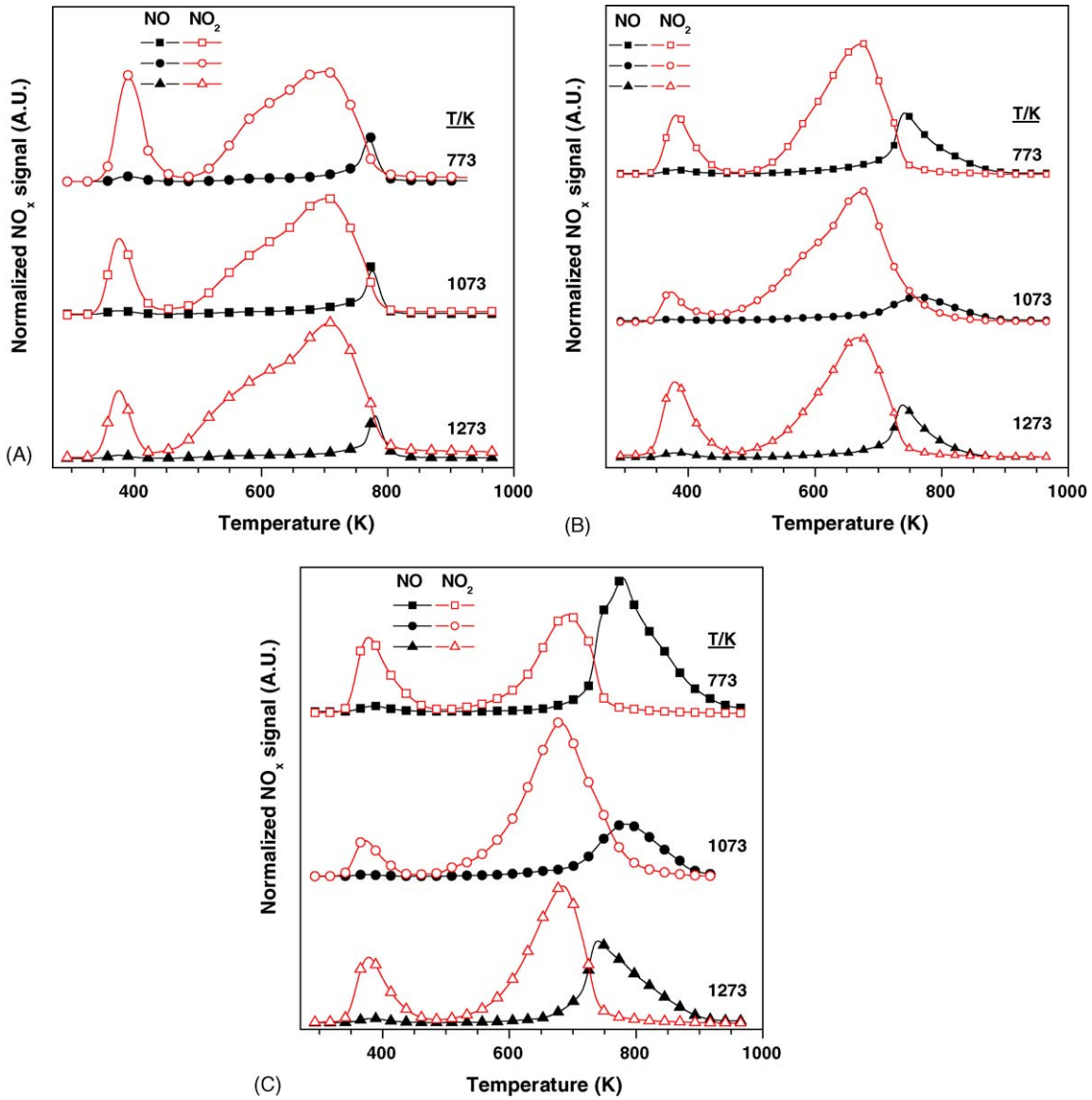

Fig. 5. TPD spectra obtained after 30 min NO_2 adsorption at room temperature on 2 wt.% (A), 8 wt.% (B), and 20 wt.% BaO/Al_2O_3 (C) catalysts after calcination at different temperatures.

positions to spectra obtained from inorganic nitrates with known structures [2]). On BaO-containing samples, IR features represent both ''bidentate'' (1300 and 1575 cm^{-1}) and ''ionic'' (1300 and 1420–1480 cm^{-1}) nitrates. In our recent studies [5], we have further clarified the nature of these nitrate species by identifying the ''ionic nitrates'' as arising from a bulk $Ba(NO_3)_2$ phase while the ''bidentate nitrates'' were assigned to surface Ba-nitrate species whose exact stoichiometry is somewhat uncertain. Bidentate nitrates are formed by the interaction of NO_2 with the monolayer BaO film on the alumina support, while bulk nitrates originate from the reaction between BaO present in excess of a monolayer and NO_2. In the data shown in Fig. 4, note especially that the relative intensity of the IR features representing the bulk (''ionic'') nitrate peaks between 1300 and 1500 cm^{-1} increase with BaO coverage. It is also clear that on the 2 and 8 wt.% BaO sample, nitrates adsorbed onto the Al_2O_3 support can be seen (as peak shoulders at ~1250 and ~1600 cm^{-1}) as well. However, these features decrease significantly with Ba loading and are essentially absent in the spectra from the 20 wt.% sample. Thus, these FT-IR results are fully consistent with the TPD results shown in Fig. 3 discussed above.

With this structural model and the corresponding interpretation of the TPD and FT-IR data in mind, we next used these techniques to study NO_2 adsorption on the higher temperature calcined samples. Upon raising the calcination temperature, only very minor changes can be seen in the TPD spectra for the cases of the 2 and 8 wt.% BaO/Al_2O_3 samples (Fig. 5A and B, respectively; these data were normalized using the BET surface areas). These results are fully consistent with the lack of morphological change observed in the XRD and TEM data for these samples with lower Ba loading. Note, however, the contrasting behavior for the 20 wt.% sample (Fig. 5C). In this case, high temperature calcination caused a significant decrease

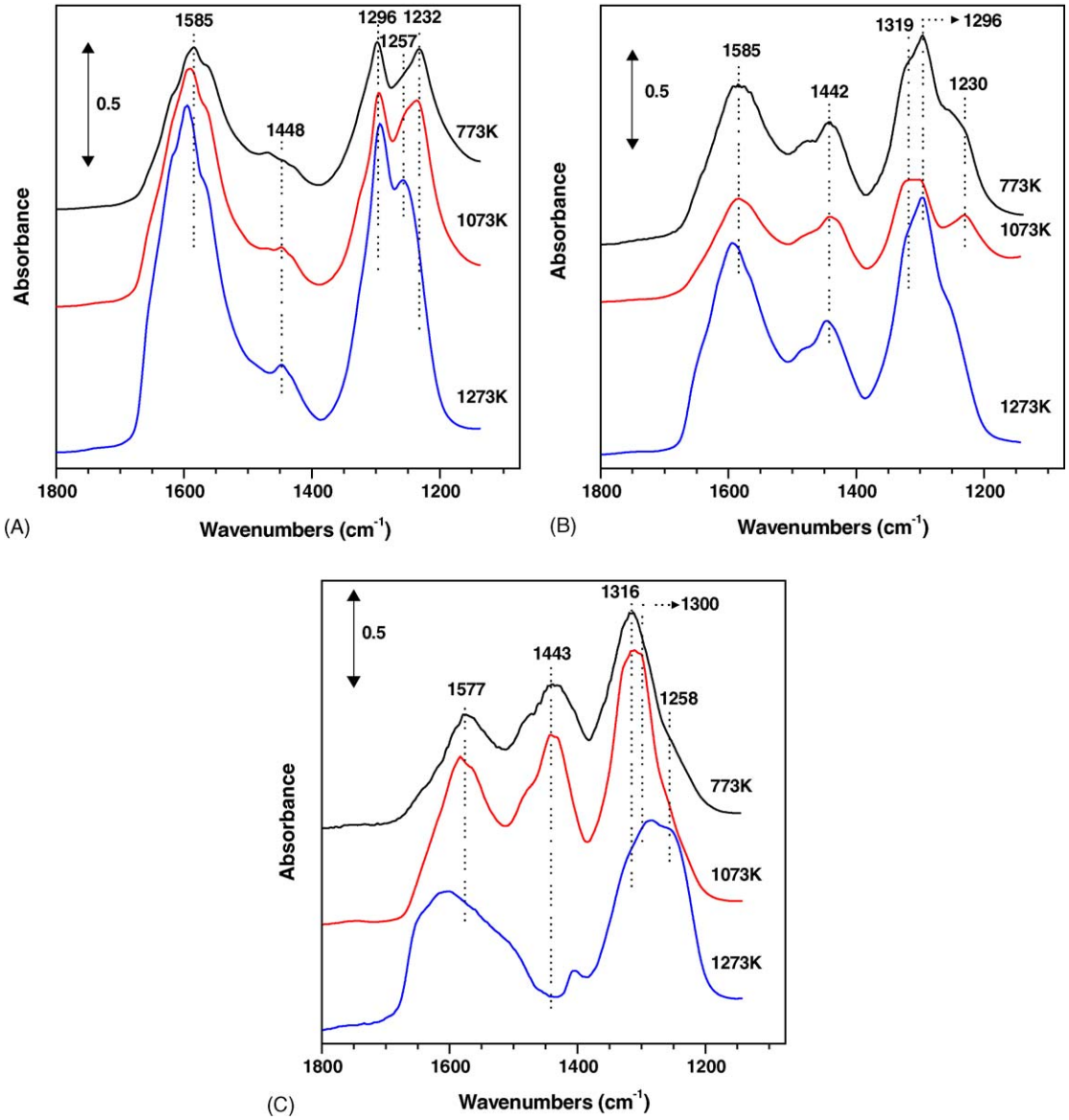

Fig. 6. IR spectra after NO_2 adsorption at room temperature on 2 wt.% (A), 8 wt.% (B), and 20 wt.% BaO/Al_2O_3 (C) catalysts after calcination to different temperatures.

in the size of the high (~800 K) temperature NO TPD peak and a corresponding increase in the lower (~700 K) temperature NO_2 peak. This suggests that the quantity of the bulk nitrate phase decreased. Since the precursor for bulk nitrate are bulk particles of BaO, these results provide further evidence that this BaO phase provides the Ba species that will undergo a solid-state reaction with alumina to produce $BaAl_2O_4$.

Still further evidence for the proposed phase changes in highly loaded NSR catalysts is provided in Fig. 6. Here again, the FT-IR spectra for the 2 and 8 wt.% samples (Fig. 6A and B, respectively) demonstrate little, if any change in the spectral region assigned for bulk (''ionic'') nitrates even after high temperature calcination. In contrast, the spectra obtained from the 20 wt.% sample (Fig. 6C), the peaks due to the bulk phase (~1445 cm^{-1}) disappear after 1273 K calcination.

4. Conclusions

Using our previous [5] model, we demonstrate from a variety of experimental techniques that we can distinguish between surface and bulk type phases of BaO supported on alumina. TEM images supported XRD results that there is no evidence for $BaAl_2O_4$ formation on 2 and 8 wt.% BaO/Al_2O_3 samples, and, moreover, that thermal ageing in air had little, if any affect on the surface BaO phase, this phase remaining intact even after a lengthy 1273 K calcination. However, for the case of higher loading, significant phase changes were observed. TEM and XRD both revealed that calcination of a 20 wt.% BaO/Al_2O_3 catalyst led to $BaAl_2O_4$ formation at temperatures as low as 1073 K. We conclude that these results demonstrate that the presence of a bulk BaO phase, i.e., more than a monolayer coverage, is required for the reaction between BaO and alumina to occur to form $BaAl_2O_4$. Consistent with this interpretation, FT-IR and NO_2 TPD results revealed that parallel with the aluminate formation the amount of bulk BaO phase declined.

Acknowledgments

The financial support of this work was provided by the U.S. Department of Energy (DOE), Office of FreedomCar and Vehicle Technologies. This work was performed in the Environmental Molecular Sciences Laboratory (EMSL) at the Pacific Northwest National Laboratory (PNNL). The EMSL is a national scientific user facility and supported by the US DOE's Office of Biological and Environmental Research. PNNL is a multi-program national laboratory operated for the U.S. DOE by Battelle Memorial Institute under contract number DE-AC06-76RLO 1830.

References

[1] W.S. Epling, L.E. Campbell, A. Yezeretz, N.W. Currier, J.E. Parks II., Catal. Rev.-Sci. Eng. 46 (2004) 163.
[2] F. Prinetto, G. Ghiotti, I. Nova, L. Lietti, E. Tronconi, P. Forzatti, J. Phys. Chem. B 105 (2001) 12732.
[3] I. Nova, L. Castoldi, L. Lietti, E. Tronconi, P. Forzatti, F. Prinetto, G. Ghiotti, J. Catal. 222 (2004) 377.
[4] P.T. Fanson, M.R. Horton, W.N. Delgass, J. Lauterbach, Appl. Catal. B 46 (2004) 393.
[5] J. Szanyi, J.H. Kwak, D.H. Kim, S.D. Burton, C.H.F. Peden, J. Phys. Chem. B 109 (2005) 27.
[6] J. Szanyi, J.H. Kwak, J. Hanson, C.M. Wang, T. Szailer, C.H.F. Peden, J. Phys. Chem. B 109 (2005) 7339.
[7] B.-H. Jang, T.-H. Yeon, H.-S. Han, Y.-K. Park, J.-E. Yie, Catal. Lett. 77 (2001) 21.
[8] M. Piacentini, M. Maciejewski, A. Baiker, Appl. Catal. B 59 (2005) 187.
[9] B. Westerberg, E. Fridell, J. Mol. Catal. A 165 (2001) 249.
[10] Ch. Sedlmair, K. Seshan, A. Jentys, J.A. Lercher, J. Catal. 214 (2003) 308.